Applied Physics A (2020) 126:284
https://doi.org/10.1007/s00339-020-03466-w

Applied Physics A
Materials Science & Processing

Development of ZnO nanostructure film for pH sensing application

Prashant Sharma[1,2] · Vijendra Singh Bhati[4] · Mahesh Kumar[5] · Rishi Sharma[2,3] · Ravindra Mukhiya[2,3] · Kamlendra Awasthi[1] · Manoj Kumar[1]

Received: 17 December 2019 / Accepted: 12 March 2020 / Published online: 19 March 2020

Abstract
Nanostructured zinc oxide sensing film was deposited on the Si/SiO_2/Pt substrate by the RF magnetron sputtering process. The film was characterized by FESEM (field-emission scanning electron microscope) and XRD (X-ray diffraction) for their morphology and structural analysis. The FESEM results show that the film morphology is in nanophase with an average nanostructure size of ~ 50 nm. XRD results show that the film is polycrystalline. The AFM (atomic force microscopy) and Raman spectroscopy were done to analyze the surface roughness and the structural properties of the film, respectively. FTIR (Fourier-transform infrared spectroscopy) was used to analyze the presence of ZnO. Further, the ZnO nanostructure film has been explored for pH sensing for pH (4–12). The sensitivity of the film was found to be 31.81 mV/pH. The drift characteristics of the film were also done to find out the stability of the film.

Keywords pH sensor · EGFET · Sensitivity · ZnO

1 Introduction

Monitoring of pH is very significant for many applications like blood pH monitoring, biological and chemical analyses, wastewater monitoring, clinical detection and many industrial applications [1–3]. Most of the pH sensors available in the market are costly, large size, bulky and hence not suitable for various biological applications. As a substitute for a glass electrode-based pH sensor, Bergveld in 1970 fabricated the ion-sensitive field-effect transistor (ISFET) [4]. The ion-sensitive field-effect transistor is quite similar to the metal–oxide–semiconductor field-effect transistor (MOSFET) with the only difference is that ISFET does not have a metal gate electrode. However, this ISFET gets affected by the chemical impurities that are present in the solution. This impurity can damage the FET as the whole device is dipped in the solution. To overcome the problem, Spiegel et al. designed and developed an alternative improved version of ISFET sensors, i.e., EGFET (Extended-Gate Field-Effect Transistor) [5]. The extended-gate field-effect transistor (EGFET), which works on the principle of ISFET, divides the original ISFET into two parts: the extended-electrode with the sensing film and the commercially available MOSFET. The MOSFET is connected to the extended-electrode where the sensing film is deposited. The EGFET has many advantages like low cost, high flexibility in terms of variation of the geometry/shape, immunity to light and temperature fluctuation, and long-term stability [6]. After the development of EGFET, several sensing films were used like TiO_2 [7], ITO [8], Na_3BiO_4–Bi_2O_3 [9], CuO [10], InN [11] for pH sensing application.

Zinc oxide in the field of semiconductors is the foremost promising candidate because of its important physical properties and application prospects. Nowadays, zinc oxide has become a popular choice for the design and development of various sensing platforms like a gas sensor, optical sensor, acoustic sensor, solar cells, biological sensor due

✉ Prashant Sharma
prashantceeri@gmail.com

✉ Manoj Kumar
mkumar.phy@mnit.ac.in

[1] Department of Physics, Malaviya National Institute of Technology Jaipur, Jaipur, Rajasthan 302017, India

[2] CSIR-Central Electronics Engineering Research Institute (CEERI), Pilani, Rajasthan 333031, India

[3] Academy of Scientific and Innovative Research (AcSIR), Ghaziabad, Uttar Pradesh 201002, India

[4] Department of Physics, Indian Institute of Technology Jodhpur, Jodhpur, Rajasthan 342017, India

[5] Department of Electrical Engineering, Indian Institute of Technology Jodhpur, Jodhpur, Rajasthan 342017, India

to its wide range of electrical and optical properties, wide bandgap (3.37 eV), high excitonic energy of 60 meV, and biocompatibility [12–17]. ZnO is an important contender for environmental and biological applications because of high mechanical strength, non-toxicity, and high reactivity. ZnO also possesses excellent electrical characteristics that can be modified by doping with different materials that are necessary for fast and accurate sensor response [18–22]. A variety of methods have been used for the synthesis and deposition of nanostructured ZnO films like hydrothermal, sol–gel, electrodeposition, chemical bath deposition, sputtering, etc. Among these deposition processes, the wet-based process is usually adopted by the researchers to prepare the ZnO nanostructure films as these processes are easy and low cost. However, these processes may cause possible unwanted impurities and defects hence incompatible with existing commercialization manufacturing technology. In our earlier work, we have developed Na_3BiO_4-Bi_2O_3 pH sensing film [9] by the electrodeposition process since this type of stoichiometry is not easy to develop by sputtering.

In this work, we have developed a biocompatible ZnO-nanostructured sensing film by the RF sputtering technique, which is a standard deposition process; it causes minimum possible impurities in the sensing film that is the most essential requirement of any commercial biological sensors. To the best of our knowledge, very few studies have been reported on the ZnO nanostructure developed by sputtering for pH sensing. The film has been characterized by using the standard techniques, and they were tested as a pH sensor.

2 Experimental details

A 4-inch silicon wafer was used as a substrate. Before deposition, the wafer was cleaned by the standard RCA cleaning process to remove any stains and contaminants from the wafer. After this, a thickness of ~ 1 µm was deposited on the silicon by the thermal oxidation process to provide the insulation. After this, Ti/Pt of thickness 200/2000 Å was deposited by the sputtering process. This layer acts as an underlying electrode. The ZnO nanostructure film of thickness ~ 350 nm was deposited by the RF sputtering system. A ZnO target (99.99% purity) was used for the deposition in the argon gas environment. The deposition process was carried out for 2 h at 1.5×10^{-2} mbar chamber pressure with an argon flow of 25 sccm. The RF power, substrate temperature, and the substrate to target distance were kept at 50 W, 400 °C, 5 cm, respectively. Structural property analyses of the nanostructure film have been carried out by X-ray diffractometer (Panalytical × Pert Pro) and Raman spectroscopy (Renishaw's inVia confocal microscope). Surface morphology and the roughness of the film were calculated by the scanning electron microscopy (Nova nano SEM FEI) and atomic force microscopy (Brucker), respectively. The purity and the presence of any function group present in the film were analyzed by Fourier transmission infrared spectroscopy (Spectrum 2Perkin Elmer). Before testing, the sensor was encapsulated by using the epoxy to prevent any leakage current keeping the sensing area open. The schematic diagram of the sensor is shown in Fig. 1. The nanostructure ZnO film was tested for pH sensing in the buffer solution 4, 6, 7, 10, and 12. The drift analysis was also done to check the stability of the sensor.

3 Results and discussions

3.1 Structural characterization

To analyze the crystal structure of the nanostructure film, XRD studies have been carried out. The XRD pattern of the ZnO nanostructure deposited on $Pt/SiO_2/Si$ substrate is shown in Fig. 2. The XRD result shows a strong (002) peak corresponding to the hexagonal wurtzite structure with preferred orientation along the c-axis [19]. The diffraction pattern fairly matches with the JCPDS Card No-01-075-0576. Sharp and intense peaks clearly show that the film is polycrystalline. The (111) peak at 39.03 is corresponding to Pt [20] which is the underlying layer and acts as an electrode.

3.2 FESEM and AFM study

The surface morphology of RF sputtered nanostructured ZnO film was studied using FESEM and is shown in Fig. 3. FESEM results show that film is uniform, nanostructure,

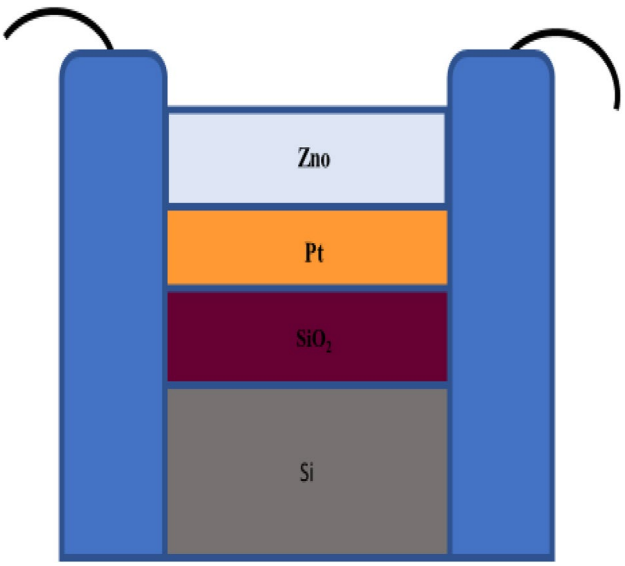

Fig. 1 A cross-sectional view of the developed extended gate with ZnO as a sensing layer for EGFET-based pH sensor

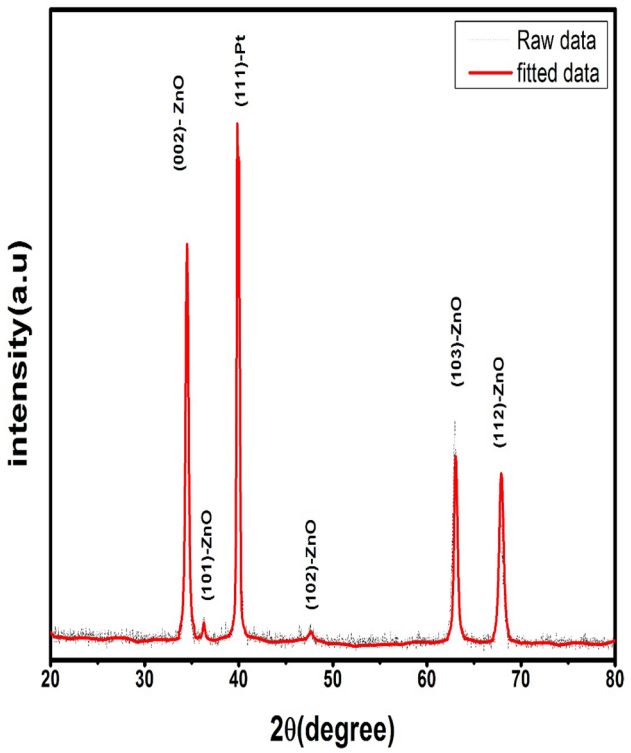

Fig. 2 XRD spectrum of ZnO-nanostructured film. The solid red line represents the profile fitted data, and the black dotted line represents the raw data

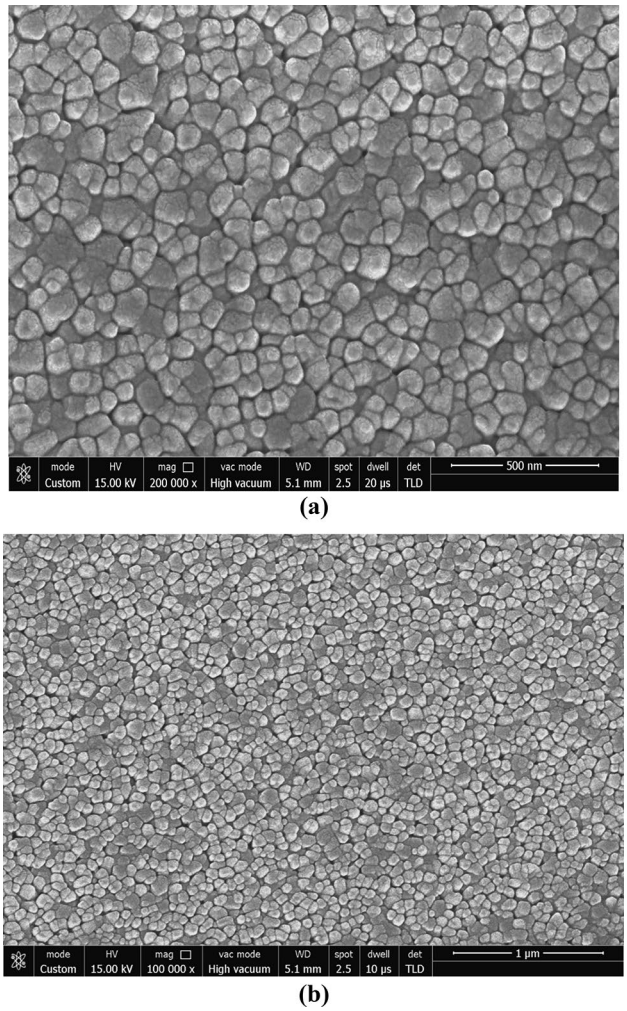

Fig. 3 FESEM image of ZnO **a** magnified view, **b** normal view

homogeneous and without any cracks. It is clear from the FESEM images that the nanostructured film is deposited on the entire Pt/Ti/SiO_2/Si substrate. The FESEM image shows that the nanostructure ZnO is grown aligned and exhibits uniform diameter, which is due to proper nucleation of the ZnO on the platinum surface (Pt/Ti/SiO_2/Si). The FESEM micrograph with 200 kx magnification and scale bar (500 nm) is shown in Fig. 3a, and the average grain size of the ZnO nanostructured film is ~ 50 nm. Figure 3b at 100 kx magnification and scale bar (1 µm) indicates the uniform morphology of the ZnO film.

Atomic force microscopy (AFM) technique was used to study the surface morphology and roughness of the ZnO film. The AFM images are taken by using the tapping mode of AFM at a scan rate of 1 Hz and are shown in Fig. 4a, b. Figure 4a shows the 2D AFM image of the ZnO film deposited on the platinum surface (Pt/Ti/SiO_2/Si) in a scan area of 2 µm × 2 µm. Figure 4b shows the 3D ZnO image in the scan area of 4 µm × 4 µm. Both 2D and 3D images of the film confirm that the deposited ZnO film is nanostructure. It is also clear from the AFM image that the film is uniformly distributed over the scan area and the surface roughness (RMS value) is found to be 5.899 nm.

FESEM and AFM analysis confirm that the film has a uniform surface morphology. The film is free from any cracks and defects that may cause leakage current during pH sensing.

3.3 Raman spectroscopy analysis

The Raman spectroscopy is an important tool to find out the structural properties and the defects present in the prepared material. The Raman spectra of the prepared film are shown in Fig. 5. The Raman analysis of the ZnO film was done by the laser of excitation wavelength 530 nm. For the wurtzite ZnO structure, the group theory (space group P63mc) infers the presence of the following optic modes: $\Gamma opt = A1 + E1 + 2E2 + 2B1$. The modes such as B1 are silent, whereas the A1 and E1 modes are polar which is infrared and Raman active. The E2 modes (E_2^{low} and E_2^{high}) are nonpolar and are only Raman active [23–26]. E_2^{low} 2 is associated with Zn sublattice, and E_2^{high} is associated with oxygen atoms [27]. B1 is the silent mode, i.e., both Raman

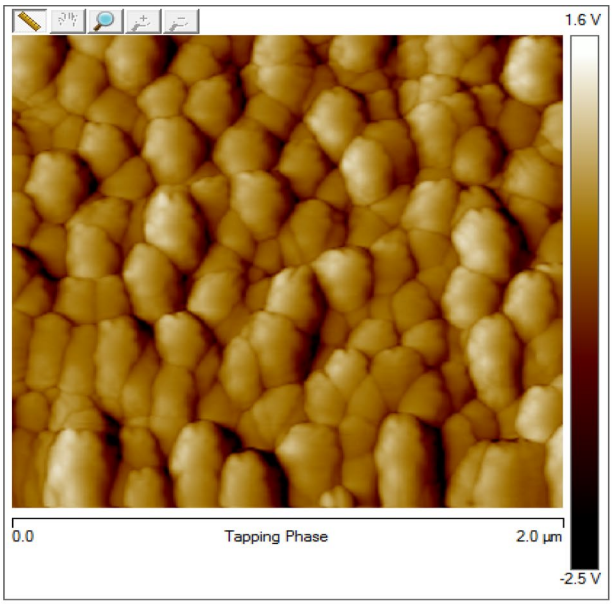

(a)

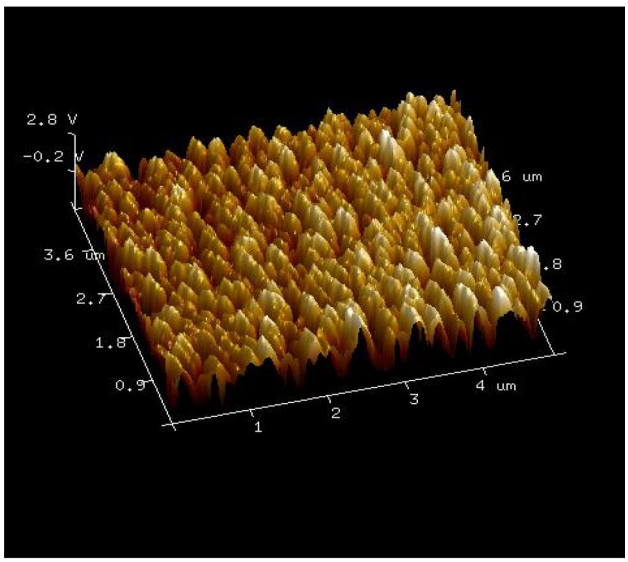

(b)

Fig. 4 AFM image of the nanostructure ZnO film **a** 2D image, **b** 3D image

and infrared inactive, whereas both A1 and E1 are infrared active and hence divided into a longitudinal and transverse optical component (LO and TO). The mode at 330 cm^{-1} is associated with the multiphonon scattering of $E_2^{high} - E_2^{low}$ [23, 28]. The most dominant and sharp peak at 437 cm^{-1} is the intrinsic Raman active mode which confirms the wurtzite structure of ZnO [29]. Hence, these results are consistent with our result obtained through XRD and confirm the formation of the ZnO wurtzite phase.

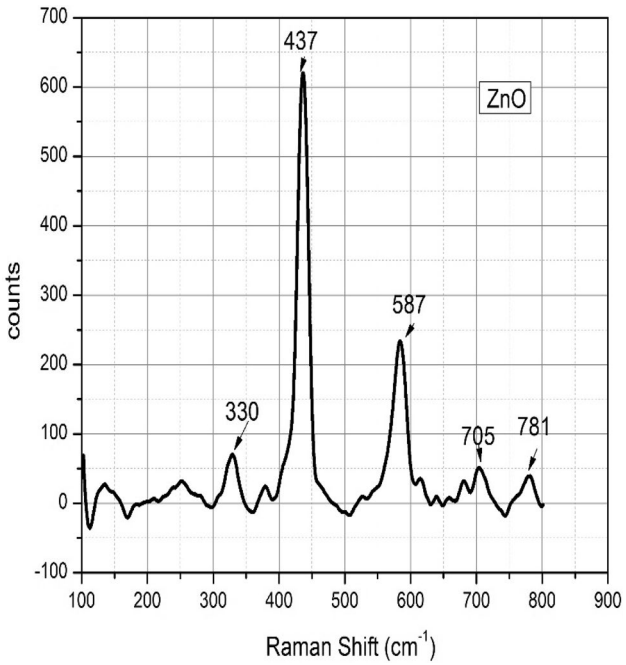

Fig. 5 Raman spectra of the ZnO nanostructure film

3.4 FTIR study

FTIR was carried out to analyze the purity and nature of the ZnO sensing film. The FTIR spectra of the sample measured in the range of 4000–400 cm^{-1} are shown in Fig. 6. The peak at 3751 cm^{-1} is due to the stretching vibration of the hydroxyl group (O–H) present at the surface. These peaks are obtained due to the absorption of moisture present in the atmosphere. A very small peak was observed at

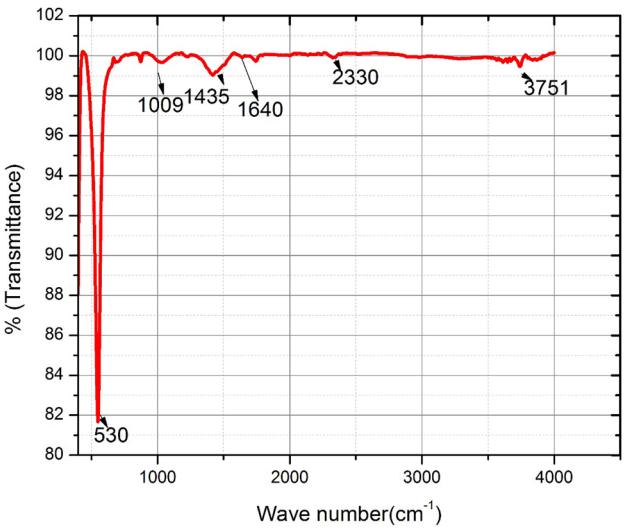

Fig. 6 FT-IR spectra of the ZnO nanostructure film

2330 cm^{-1}, and this peak corresponds to CO_2 mode [30]. This mode is due to the atmospheric CO_2 present in the sample and not because of any serious contamination. Samples might have absorbed some CO_2 from the environment during FTIR measurement. The infrared bands present in the region between 1700–600 cm^{-1} (see Fig. 6) correspond to the C=O, C–O, and C–H vibrations, respectively [31]. The peak at 530 cm^{-1} is due to the Zn–O stretching vibrations, and it confirms the presence of ZnO [32, 33]. The presence of ZnO is also confirmed by XRD and Raman characterization techniques.

3.5 Electrical characterization

To investigate the sensing performance of the nanostructure, ZnO-based EGFET sensor in different pH solutions constant current (I_{ds}) and constant voltage (V_{ds}) measurements was taken by changing the reference voltage (V_{ref}). The setup is completed with a commercial CD4007UB MOSFET. The details of the whole set up are available in our previous report [9]. The transfer characteristics of the sensor are shown in Fig. 7. For pH sensing, the reference electrode and the sensing chip were immersed in the pH buffer solution 4, 6, 7, 10, and 12, respectively. The sensitivity of the sensor was evaluated from the linear fit (Fig. 8). The sensitivity was found to be 31.81 mV/pH. The sensitivity depends upon the number of binding sites (N_s), which depends upon the morphology of the film. The principle of measurement of pH sensing is explained by the site-binding model [34, 35]. The

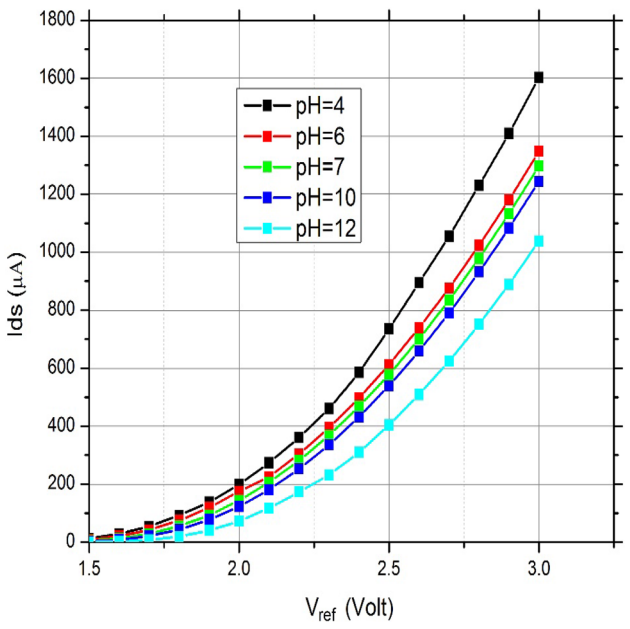

Fig. 7 Transfer characteristics of the ZnO-nanostructure-based EGFET pH sensor

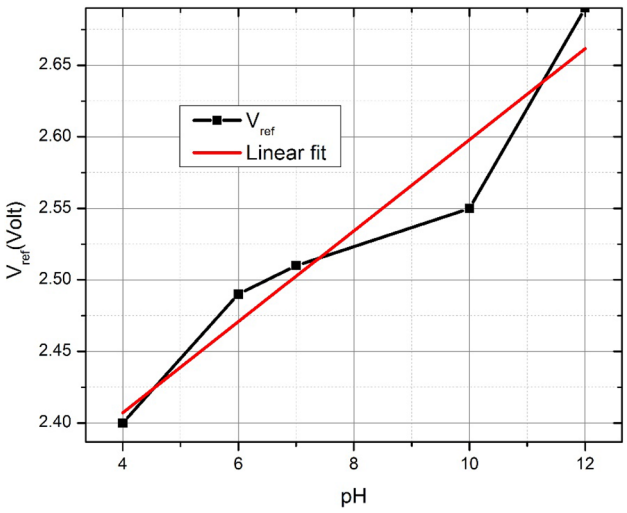

Fig. 8 pH vs V_{ref} for ZnO-nanostructure-based EGFET pH sensor

surface potential (Ψ_0) generated between the electrolyte and the sensing layer can be expressed as (Eq. 1) [36]

$$2.303\left(\mathrm{pH}_{\mathrm{pzc}} - \mathrm{pH}\right) = \frac{q\Psi}{kT} + \sinh^{-1}\frac{q\Psi}{kT}\cdot\frac{1}{\beta} \tag{1}$$

where pH_{pzc} is the pH value at the point of zero charge, T is the absolute temperature, q is the electron charge, k is the Boltzmann constant, and β is the intrinsic buffer capacity. The relation between the number of surface sites per unit area (N_s) and β is given by Eq. 2.

$$\beta = \frac{2q^2 N_s \left(K_a K_b\right)^{\frac{1}{2}}}{KTC_{DL}} \tag{2}$$

where K_a and K_b are acid and base equilibrium constants, respectively, and C_{DL} is the capacitance due to the electrical double layer derived from the Gouy–Chapman–Stern–Graham model [37].

3.6 Sensing mechanism

The sensing mechanism of ZnO film, as a pH sensing layer on EGFET, is based on the site-binding model given by Yates et al. [34]. ZnO is an inorganic metal oxide which has amphoteric surface sites. These sites can either donate or accept protons when it is dipped in an electrolyte. The ZnO surface contains the hydroxyl groups. These hydroxyl groups adsorbed the hydroxyl ion when coming in contact with the electrolyte and form a positive or negative charge at the surface. In alkaline medium, the chemisorbed protons dissociate from the surface and leave the surface negatively charged, whereas in the acidic medium the protons from the environment react with the surface and make the surface

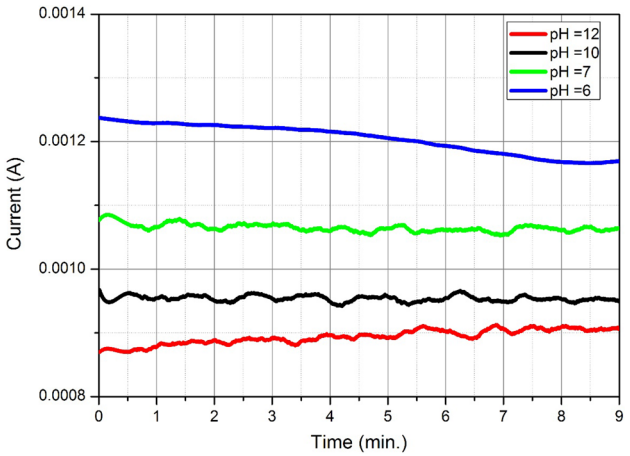

Fig. 9 Drift characteristics of the ZnO-nanostructured EGFET pH sensor

positively charged. The surface charge developed at the surface can be expressed by the following reaction [38, 39].

$$ZnO_{(s)} + 2H_2O = Zn(OH)^{-}_{3(s)} + H^{+}(\text{alkaline})$$

$$ZnO_{(s)} + H^{+} = Zn(OH)^{+}_{(s)}$$

3.7 Stability analysis of the nanostructured film during pH sensing

The long-term stability analysis of the sensor for the proper functioning of the sensor, the drift characteristic was also done. The measurement was taken for both acidic and basic pH values. The sensor was dipped in the different pH buffer solution with $V_{DS} = 2.5$ V and $V_{ref} = 2.5$ V, and the currents were measured. The drift characteristic of the nanostructured ZnO EGFET sensor is shown in Fig. 9. The sensor shows good stability results with a very small drift. The sensor can be proposed to be used in various biological pH sensing applications.

4 Conclusions

Nanostructure ZnO film has been developed by the RF sputtering process. The film was deposited on the Pt/SiO_2/Si substrate. The film was analyzed as a sensing film for the EGFET-based pH sensor. XRD and Raman results show that the ZnO film is polycrystalline in nature and wurtzite structure. FESEM and AFM study confirms that the film is nanostructured. These nanostructured sensing films were characterized for pH sensing in the buffer solution of pH 4, 6, 7, 10, and 12. The sensitivity of the film was found to be 31.81 mV/pH. The drift analysis was also done to find the long-term stability of the film. The film showed very small drift changes and found suitable for pH sensing applications. The developed EGFET sensor with ZnO sensing film that is biocompatible can be proposed for various pH sensing applications in the biomedical area.

Acknowledgements The authors acknowledge IIT, Jodhpur for extending the experimental facility, and MRC, MNIT Jaipur for characterization facilities. Authors are also thankful to CSIR, New Delhi for providing the research facilities and financial support. They also acknowledge the support of Director, CSIR-CEERI, Pilani.

References

1. Q. Zhang, K. Zhang, D. Xu, G. Yang, H. Huang, F. Nie, C. Liu, S. Yang, CuO nanostructures: synthesis, characterization, growth mechanisms, fundamental properties, and applications. Prog. Mater Sci. **1**(60), 208–337 (2014)
2. Q. Shao, R.H. Que, M.W. Shao, Q. Zhou, D.D. Ma, S.T. Lee, Shape controlled flower-like silicon oxide nanowires and their pH response. Appl. Surf. Sci. **257**(13), 5559–5562 (2011)
3. X. Fang, T. Zhai, U.K. Gautam, L. Li, L. Wu, Y. Bando, D. Golberg, ZnS nanostructures: from synthesis to applications. Prog. Mater Sci. **56**(2), 175–287 (2011)
4. P. Bergveld, Development of an ion-sensitive solid-state device for neurophysiological measurements. IEEE Trans. Biomed. Eng. **1**, 70–71 (1970)
5. I. Lauks, P. Chan, D. Babic, The extended gate chemically-sensitive field effect transistor as multi-species microprobe. Sens. Actuators **4**, 291–298 (1983)
6. S.A. Pullano, C.D. Critello, I. Mahbub, N.T. Tasneem, S. Shamsir, S.K. Islam, M. Greco, A.S. Fiorillo, EGFET-based sensors for bioanalytical applications: a review. Sensors. **18**(11), 4042 (2018)
7. J.Y. Li, S.P. Chang, S.J. Chang, T.Y. Tsai, Sensitivity of EGFET pH sensors with TiO_2 nanowires. ECS Solid State Lett. **3**(10), 123–126 (2014)
8. Q. Li, H. Li, J. Zhang, Z. Xu, A novel pH potentiometric sensor based on electrochemically synthesized polybisphenol A films at an ITO electrode. Sens. Actuators B Chem. **155**(2), 730–736 (2011)
9. P. Sharma, S. Gupta, R. Singh, K. Ray, S.L. Kothari, S. Sinha, R. Sharma, R. Mukhiya, K. Awasthi, M. Kumar, Hydrogen ion sensing characteristics of Na_3BiO_4–Bi_2O_3 mixed oxide nanostructures based EGFET pH sensor. Int. J. Hydrog. Energy. (2019). https://doi.org/10.1016/j.ijhydene.2019.07.252
10. S.P. Chang, T.H. Yang, Sensing performance of EGFET pH sensors with CuO nanowires fabricated on glass substrate. Int. J. Electrochem. Sci. **7**, 5020–5027 (2012)
11. S.X. Chen, S.P. Chang, S.J. Chang, Investigation of InN nanorod-based EGFET pH sensors fabricated on quartz substrate. Dig. J. Nanomater. Biostruct. **9**, 1505–1511 (2014)
12. A. Janotti, C.G. Van de Walle, Fundamentals of zinc oxide as a semiconductor. Rep. Prog. Phys. **72**(12), 126501 (2009)
13. K. Hara, T. Horiguchi, T. Kinoshita, K. Sayama, H. Sugihara, H. Arakawa, Highly efficient photon-to-electron conversion with mercurochrome-sensitized nanoporous oxide semiconductor solar cells. Sol. Energy Mater. Sol. Cells **64**(2), 115–134 (2000)
14. J.I. Oda, J.I. Nomoto, T. Miyata, T. Minami, Improvements of spatial resistivity distribution in transparent conducting Al-doped ZnO thin films deposited by DC magnetron sputtering. Thin Solid Films **518**(11), 2984–2987 (2010)
15. Yen WT, Ke JH, Wang HJ, Lin YC, Chiang JL, in *Influences on optoelectronic properties of damp heat stability of AZO and GZO*

for thin film solar cells. Advanced Materials Research 2009, vol. 79 (Trans Tech Publications), pp. 923–926
16. Y. Liu, M. Zhong, G. Shan, Y. Li, B. Huang, G. Yang, Biocompatible ZnO/Au nanocomposites for ultrasensitive DNA detection using resonance Raman scattering. J. Phys. Chem. B **112**(20), 6484–6489 (2008)
17. M. Tak, V. Gupta, M. Tomar, Flower-like ZnO nanostructure based electrochemical DNA biosensor for bacterial meningitis detection. Biosens. Bioelectron. **15**(59), 200–207 (2014)
18. H.C. Pan, M.H. Shiao, C.Y. Su, C.N. Hsiao, Influence of sputtering parameter on the optical and electrical properties of zinc-doped indium oxide thin films. J. Vac. Sci. Technol., A **23**(4), 1187–1191 (2005)
19. X. Zhang, Z. Dong, S. Liu, Y. Shi, Y. Dong, W. Feng, Maize straw-templated hierarchical porous ZnO: Ni with enhanced acetone gas sensing properties. Sens. Actuators B Chem. **1**(243), 1224–1230 (2017)
20. X. Zhao, Y. Li, C. Ai, D. Wen, Resistive switching characteristics of li-doped ZnO thin films based on magnetron sputtering. Materials. **12**(8), 1282 (2019)
21. S. Singh, A. Singh, R.R. Yadav, P. Tandon, Growth of zinc ferrite aligned nanorods for liquefied petroleum gas sensing. Mater. Lett. **15**(131), 31–34 (2014)
22. A.K. Jaiswal, S. Singh, A. Singh, R.R. Yadav, P. Tandon, B.C. Yadav, Fabrication of Cu/Pd bimetallic nanostructures with high gas sorption ability towards development of LPG sensor. Mater. Chem. Phys. **15**(154), 16–21 (2015)
23. K.A. Alim, V.A. Fonoberov, M. Shamsa, A.A. Balandin, Micro-Raman investigation of optical phonons in ZnO nanocrystals. J. Appl. Phys. **97**(12), 124313 (2005)
24. S.B. Yahia, L. Znaidi, A. Kanaev, J.P. Petitet, Raman study of oriented ZnO thin films deposited by sol–gel method. Spectrochim. Acta Part A Mol. Biomol. Spectrosc. **71**(4), 1234–1238 (2008)
25. D.L. Golic, G. Brankovic, M.P. Nešic, K. Vojisavljevic, A. Recnik, N. Daneu, S. Bernik, M. Ščepanovic, D. Poleti, Z. Brankovic, Structural characterization of self-assembled ZnO nanoparticles obtained by the sol–gel method from Zn (CH3COO) 2 2H2O. Nanotechnology. **22**(395603), 9 (2011)
26. R. Cuscó, E. Alarcón-Lladó, J. Ibanez, L. Artús, J. Jiménez, B. Wang, M.J. Callahan, Temperature dependence of Raman scattering in ZnO. Phys. Rev. B. **75**(16), 165202 (2007)
27. Calizo I, Alim KA, Fonoberov VA, Krishnakumar S, Shamsa M, Balandin AA, Kurtz R, in *Micro-Raman spectroscopic characterization ZnO quantum dots, nanocrystals, and nanowires*. Quantum Dots, Particles, and Nanoclusters IV 2007, vol 6481. International Society for Optics and Photonics, p. 64810 N
28. S.S. Kanmani, K. Ramachandran, S. Umapathy, Eosin yellowish dye-sensitized ZnO nanostructure-based solar cells employing solid PEO redox couple electrolyte. Int. J. Photoenergy (2012). https://doi.org/10.1155/2012/267824
29. M. Rajalakshmi, A.K. Arora, B.S. Bendre, S. Mahamuni, Optical phonon confinement in zinc oxide nanoparticles. J. Appl. Phys. **87**(5), 2445–2448 (2000)
30. B.N. Dole, V.D. Mote, V.R. Huse, Y. Purushotham, M.K. Lande, K.M. Jadhav, S.S. Shah, Structural studies of Mn doped ZnO nanoparticles. Curr. Appl. Phys. **11**(3), 762–766 (2011)
31. K.S. Babu, A.R. Reddy, C. Sujatha, K.V. Reddy, A.N. Mallika, Synthesis and optical characterization of porous ZnO. J. Adv. Ceram. **2**(3), 260–265 (2013)
32. M. Khan, A.H. Naqvi, M. Ahmad, Comparative study of the cytotoxic and genotoxic potentials of zinc oxide and titanium dioxide nanoparticles. Toxicol. Rep. **1**(2), 765–774 (2015)
33. K. Khun, Z.H. Ibupoto, M.S. AlSalhi, M. Atif, A.A. Ansari, M. Willander, Fabrication of well-aligned ZnO nanorods using a composite seed layer of ZnO nanoparticles and chitosan polymer. Materials **6**(10), 4361–4374 (2013)
34. D.E. Yates, S. Levine, T.W. Healy, Site-binding model of the electrical double layer at the oxide/water interface. J. Chem. Soc. Faraday Trans. Phys. Chem. Condens. Phases. **70**, 1807–1818 (1974)
35. R.E. Van Hal, J.C. Eijkel, P. Bergveld, A novel description of ISFET sensitivity with the buffer capacity and double-layer capacitance as key parameters. Sens. Actuators B Chem. **24**(1–3), 201–205 (1995)
36. H.K. Liao, L.L. Chi, J.C. Chou, W.Y. Chung, T.P. Sun, S.K. Hsiung, Study on pHpzc and surface potential of tin oxide gate ISFET. Mater. Chem. Phys. **59**(1), 6–11 (1999)
37. K.B. Oldham, A Gouy–Chapman–Stern model of the double layer at a (metal)/(ionic liquid) interface. J. Electroanal. Chem. **613**(2), 131–138 (2008)
38. S. Al-Hilli, R. Al-Mofarji, P. Klason, N. Gutman, A. Sa'Ar, A. Ost , P. Stralfors, M. Willander. Zinc oxide nanorods as an intracellular pH sensor, European Nano Systems (ENS) Worshop, Paris, France, 03–04 December 2007, pp. 38–43
39. A. Wei, L. Pan, W. Huang, Recent progress in the ZnO nanostructure-based sensors. Mater. Sci. Eng., B **176**(18), 1409–1421 (2011)